

Gamma-ray lens development status for a European Gamma-Ray Imager

F. Frontera^{a,d}, A. Pisa^a, V. Carassiti^b, F. Evangelisti^b, G. Loffredo^a, D. Pellicciotta^a, K.H. Andersen^c, P. Courtois^c, L. Amati^d, E. Caroli^d, T. Franceschini^d, G. Landini^d, S. Silvestri^d, J.B. Stephen^d

^aUniversity of Ferrara, Physics Department, Via Saragat 1, 44100 Ferrara, Italy;

^bIstituto Nazionale Fisica Nucleare, Sezione di Ferrara, Via Saragat 1, 44100 Ferrara, Italy;

^cInstitute Laue-Langevin, 6 Rue Jules Horowitz, 38042 Grenoble, France ^dINAF, IASF Bologna, Via Gobetti 101, 40129 Bologna, Italy

ABSTRACT

A breakthrough in the sensitivity level of the hard X-/gamma-ray telescopes, which today are based on detectors that view the sky through (or not) coded masks, is expected when focusing optics will be available also in this energy range. Focusing techniques are now in an advanced stage of development. To date the most efficient technique to focus hard X-rays with energies above 100 keV appears to be the Bragg diffraction from crystals in transmission configuration (Laue lenses). Crystals with mosaic structure appear to be the most suitable to build a Laue lens with a broad passband, even though other alternative structures are being investigated. The goal of our project is the development of a broad band focusing telescope based on gamma-ray lenses for the study of the continuum emission of celestial sources from 60 keV up to >600 keV. We will report details of our project, its development status and results of our assessment study of a lens configuration for the European Gamma Ray Imager (GRI) mission now under study for the ESA plan Cosmic Vision 2015-2025.

Keywords: Laue lenses, gamma-ray instrumentation, focusing telescopes, gamma-ray observations

1. INTRODUCTION

As demonstrated by the long history of astronomy, any progress in the knowledge of the sky is strictly correlated with an increase in the instrument sensitivity. In hard (>10 keV) X-ray astronomy, focusing telescopes now under development are expected to provide a big leap in our knowledge of the high energy astrophysical phenomena. While below 100 keV X-ray optics based on multilayer coatings (ML) appears to be the best technique to build hard X-ray mirrors, above 100 keV the best candidate technique at the present time appears the Bragg diffraction from crystals in transmission configuration (Laue lenses).

A huge increase in sensitivity (by a factor 10–100) above 100 keV would open a new window of investigation, with the concrete possibility of fixing many open issues, apart from the prospect of unexpected discoveries. Among the open issues which can be fixed only with high energy (> 100 keV) observations, we mention (see Frontera et al.¹):

- Origin and physics of the high energy cut-offs of type 1 and type 2 Active Galactic Nuclei (AGNs);
- Contribution of (thermal and non-thermal) AGNs to the high energy Cosmic X-/gamma-ray background (CXB). Synthesis models require a spectral roll-over with an e-folding energy of 100-400 keV in AGNs. So far only a few sparse measurements are available.
- Role of the antimatter in the Universe from the study of the $e^+ - e^-$ pair annihilation line and the effect on it of strong gravitational fields;

Further author information: (Send correspondence to F.F.)

F.F: E-mail: frontera@fe.infn.it, Telephone: +39 0532 974 254

- Role of non thermal mechanisms in extended objects (Supernova remnants, Galaxy clusters);
- Properties of the high energy emission in presence of super-strong ($> 10^{13}$ G) magnetic fields (mass accreting X-ray pulsars, anomalous X-ray pulsars, Soft Gamma-Ray Repeaters);
- Role of Comptonization in compact mass accreting objects and in Gamma Ray Bursts;
- Study the star explosion mechanisms via the detection of the nuclear lines from synthesized elements (e.g., Co, Ni, Ti);

Here we give the status of our HAXTEL (= HARd X-ray TELEscope) project devoted to develop Laue lenses for the study of the continuum spectra from 60 to 600 keV. This development is complementary to that which is being performed by other groups,² devoted to the development of Laue lenses for the study of nuclear gamma-ray lines. All these studies will be usefully exploited for the study of a Gamma Ray Imager (GRI) mission now under study to be submitted to the European Space Agency (ESA) for its mission plan "Cosmic Vision 2015-2025".

2. RESULTS OBTAINED SO FAR

Results of the activity performed thus far are the subject of various papers.³⁻⁵ They concern a theoretical feasibility study devoted to establish the best design of a Laue lens telescope along with its sensitivity expectations,^{3,4} Monte Carlo simulations of the expected optical properties of Laue lenses, reflectivity measurements of mosaic crystal samples of Cu(111).⁵ Here we summarize the most relevant results.

2.1. Results from a feasibility study

This study was performed through calculations. The Laue lens of our project is requested to have a spherical shape with radius R and focal length $f = R/2$. Assuming flat crystals, in order to get the best approximation of the lens geometry, crystal tiles with small facets are required (of the order of 10×10 mm²).

Perfect crystals are not suitable for building lenses for astrophysical investigations. Indeed they show a high reflection efficiency but in a very narrow energy band (of the order of a few eV). Given that we have to cover with good reflection efficiency a relatively broad energy band (several hundreds of keV), special crystals, with properly controlled lattice deformations, appear to be more useful. Crystals of this kind include mosaic crystals, bent crystals and crystals with non constant lattice spacing d induced by doping materials or thermal gradients. For our project we have assumed mosaic crystals, made of crystallites misaligned each with other with controlled angular spread β (FWHM of the Gaussian-like angular distribution of the crystallite misalignments). The growing technique of mosaic crystals with the desired spread is now being consolidated (e.g., Courtois et al.⁸). In the case of a mosaic crystal, when a polychromatic parallel beam of X-rays impinges on it with mean Bragg angle θ_B , from the Bragg law ($2d \sin \theta_B = n \frac{hc}{E}$, where the Bragg angle θ_B is the angle between the lattice planes and the direction of the incident and diffracted photons, $n = 1, 2, ..$ is the diffraction order, E in keV units is the photon energy and $hc = 12.4$ keV·Å if d is given in Å), photons in a bandwidth

$$\Delta E = E \beta / \tan \theta_B \quad (1)$$

are reflected by the mosaic crystal.

Crystal tiles of thickness t are assumed to have their mean lattice plane normal to the tile main facets, which are assumed to be square of side l .

To correctly focus photons (see Fig. 1), the direction of the vector perpendicular to the mean lattice plane of each crystal has to intersect the lens axis and its inclination with respect to the focal plane has to be equal to the Bragg angle θ_B . The angle θ_B depends on the distance r of the tile center from the lens axis and on the focal length f . For a correct focusing, it is needed that $\theta_B = 1/2 \arctan(r/f)$. Once the crystal material is established, the Bragg angle increases with r/f , while the energy of the focused photons decreases with r/f . More generally, once the focal length is established, the outer and inner lens radii, r_{max} and r_{min} (see Fig. 1),

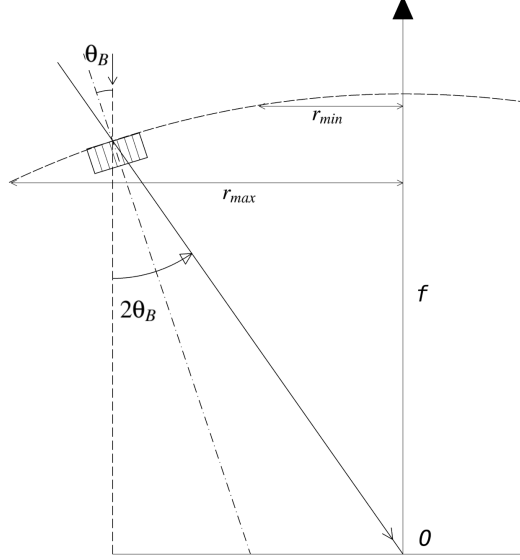


Figure 1. Scheme of the Bragg diffraction in a Laue lens. The X-ray photons in a given energy band ΔE around E , which impinge on the lens parallel to the z axis (lens axis), are diffracted only by those mosaic crystals oriented in such a way as to satisfy Eq. 1. The photons with centroid energy E which hit the center of these crystals are focused in the lens focus (point O), r_{max} and r_{min} define the innermost and outermost radius of the lens surface, respectively. Reprinted from.⁵

depend on the nominal energy passband of the lens (E_{min} , E_{max}) according to the following equation, derived from the Bragg law:

$$\begin{aligned} r_{max} &\approx 12.4 \frac{f_{100}}{d_{hkl}(\text{\AA}) E_{100}} m \\ r_{min} &\approx 1.24 \frac{f_{100}}{d_{hkl}(\text{\AA}) E_{1000}} m \end{aligned} \quad (2)$$

where f_{100} is the focal length in units of 100 m, $d_{hkl}(\text{\AA})$ is the spacing of the lattice planes with Miller indices (h,k,l) in units of \AA , and E_{100} and E_{1000} is the photon energy in units of 100 keV and 1000 keV, respectively.

From the previous equation, it is possible to see that the lens radii not only depend on the energy passband, but also on the crystal lattice spacing: higher d_{hkl} implies lower radii.

Among the candidate materials for their high reflectivity, Cu (111) appears very promising for the hard X-/gamma-ray range (see Fig. 2). It is indeed one of the few materials for which the technology for its growing with mosaic structure has already been developed with good results (see below).

For a fixed inner and outer radius, the lens passband and its effective area can be further controlled by the use of a combination of different crystal materials. Mosaic spread and, for a fixed material, crystal thickness are the most crucial parameters to be fixed to optimize the lens performance.

The effect of the crystal thickness on the lens effective area has been discussed in previous papers (see, e.g., Pisa et al.³). It results that a single thickness is not the best solution for optimizing the lens effective area in its entire passband. However the optimization of the lens effective area at the highest energies could imply large thicknesses, that could be incompatible with lens weight constraints. We have investigated this issue elsewhere,⁶ finding that a decrease in the thickness of the order of 25% with respect to the optimized value results in a very small decrease of the effective area, while the lens weight significantly decreases.

Also the mosaic spread β (see Eq. 1) affects the lens performance. A higher spread gives a larger effective area,³ but also produces a larger defocusing of the reflected photons in the focal plane, as can be seen in Fig. 3,

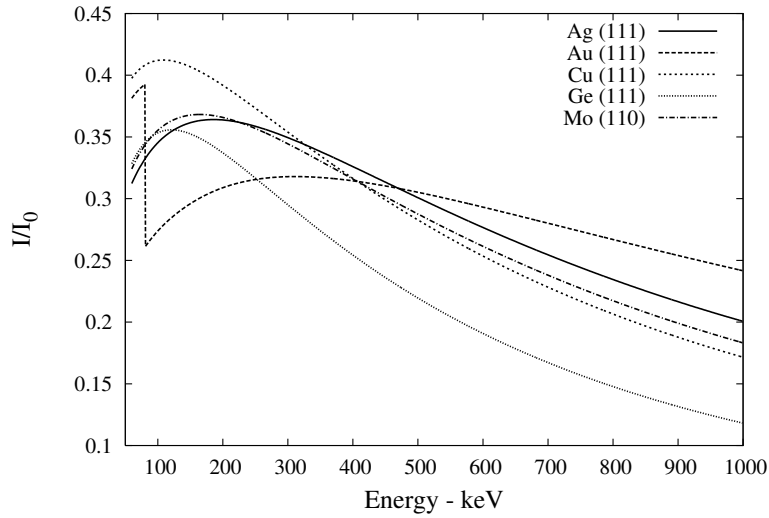


Figure 2. Peak reflectivity of 5 candidate crystal materials. The Miller indices used give the highest reflectivity. A mosaic spread of 40 arcsec is assumed. The production technology of mosaic crystals with the required spread has currently been developed only for Ge and Cu.

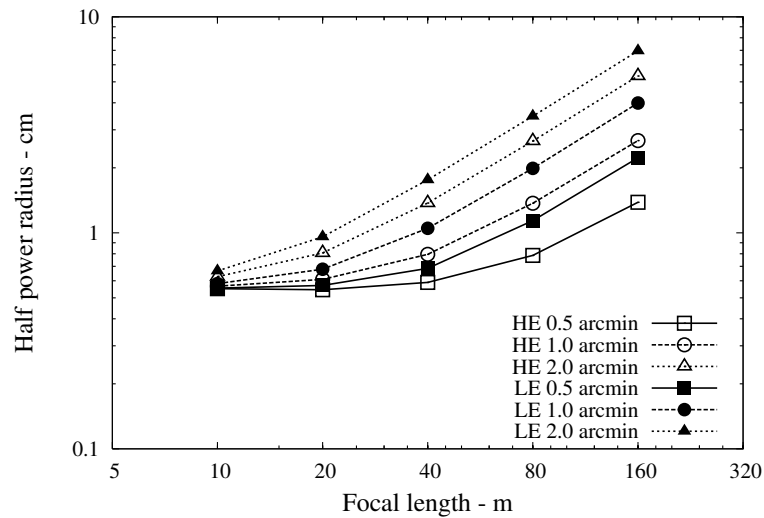


Figure 3. Radius of the circle in which are focused 50% of the reflected photons (Half Power Radius, HPR) as a function of the focal distance, for various values of the mosaic spread in two energy bands, 90–110 keV (LE), and 450–550 keV (HE).

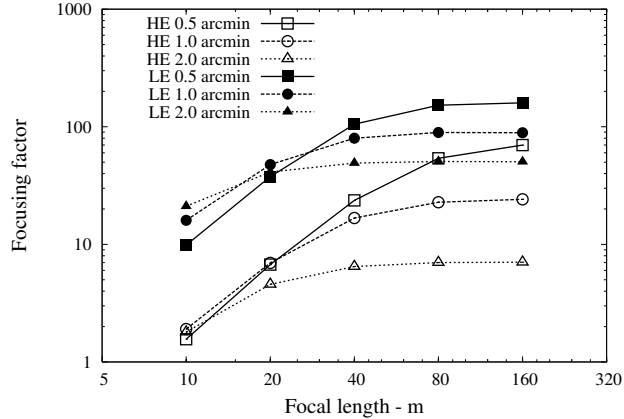


Figure 4. Dependence of the focusing factor G on the focal length F for three different values of the mosaic spread in two different energy bands: 90–110 keV (LE) and 450–550 keV (HE). See text.

in which we show how the radius of the circle which contains 50% of the reflected photons in the focal plane (Half Power Radius, HPR) changes with the focal length for various values of the mosaic spread.

The best parameter which takes into account both the effective area and the size of the focal spot in the focal plane is the focusing factor G , which is given by:

$$G = f_{ph} \frac{A_{eff}}{A_d} \quad (3)$$

in which A_{eff} is the effective area of the lens and A_d is the area of the focal spot which contains a fraction f_{ph} of photons reflected by the lens. From the expression of the lens sensitivity to the continuum emission

$$I_{min}(E) = \frac{n_\sigma}{\eta_d A_{eff} f_{ph}} \sqrt{\frac{2BA_d}{T \Delta E}} \quad (4)$$

where I_{min} (photons $\text{cm}^{-2} \text{s}^{-1} \text{keV}^{-1}$) is the the minimum detectable intensity in the interval ΔE around E , n_σ is the significance level of the signal (typically $n_\sigma = 3-5$), B is the focal plane detector background intensity (counts $\text{cm}^{-2} \text{s}^{-1} \text{keV}^{-1}$), T is exposure time to a celestial source, and η_d is the focal plane detector efficiency at energy E , it can be seen that the lens sensitivity is inversely proportional to G .

We have investigated⁷ the dependence of G on the focal length for three values of the mosaic spread (0.5, 1 and 2 arcmin) and for two different lens passbands: 90–110 keV (Low Energy, LE) and 450–550 keV (High Energy, HE). For $f_{ph} = 0.50$ corresponding to the HPR and for crystal tiles of $15 \times 15 \text{ mm}^2$, we find the result shown in Fig. 4. As can be seen, G is significantly higher at low energies, shows a saturation for high focal lengths, and, specially at high energies, significantly increases with the spread decrease. However, compatibly with an acceptable G , a larger spread would be preferred, since it gives a higher effective area and thus a higher photon collection. In addition, a larger spread requires a lower accuracy in the positioning of the crystals in the lens.³

Another issue we have investigated is the disposition of the mosaic crystal tiles in the lens for a uniform coverage of the lens passband. The result is that the best crystal tile disposition is that of an Archimedes' spiral. This disposition^{3,5} is crucial to get a smooth change of the lens effective area A_{eff} with energy, apart from the jumps due to diffraction orders higher than one. However the Archimedes' spiral becomes less important for high focal lengths ($> 30 \text{ m}$).

The advantage of the Laue lenses with respect to the direct-viewing telescopes, is better illustrated by the equivalent effective area S , defined, in the case of a lens, as $S = G^2 A_d$, while, in the case of a direct-viewing

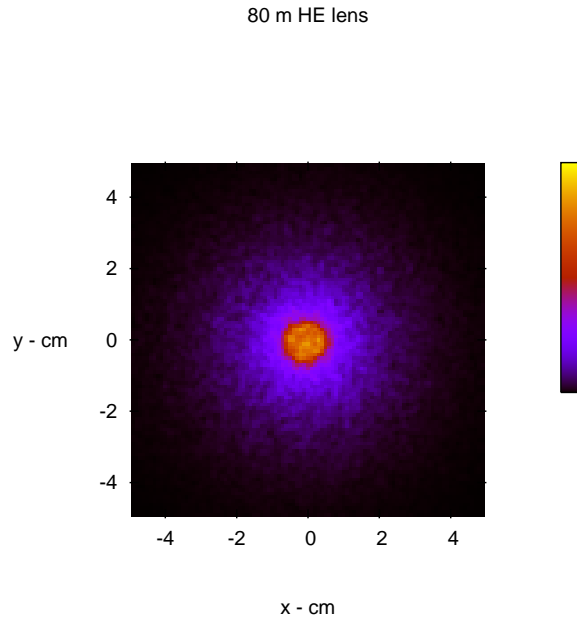


Figure 5. Point spread function of a lens with 80 m focal length for an on-axis source in the 150–600 keV energy band.

telescope, S is the useful detector area. In both cases the sensitivity (see eq. 4) is inversely proportional to $S^{0.5}$, but for the lenses it is proportional to G and thus increases with the focal length (see Fig. 4).

Special care has to be taken in the accuracy of the crystal tile positioning in the lens. A deviation of the crystal orientation with respect to the nominal position degrades the focusing factor. The accuracy required in the crystal tile positioning to get a negligible degradation not only depends on the mosaic spread, as above mentioned, but also on the focal length. Higher focal lengths require higher positioning accuracies, which is at the current stage of development one of the major problems to be faced for the realization of a Laue lens.

2.2. Results from Monte Carlo simulations

A Monte Carlo (MC) code has been developed by us to derive the properties of different lens configurations for either on-axis and off-axis incident photons. For a ring of square crystal tiles of $10 \times 10 \text{ mm}^2$ cross section and 2 mm thickness, properly oriented for 150 keV photons, the MC results have already been reported.⁶ They confirm the results obtained from the theoretical investigation and extend them. Among the results obtained (some of them already mentioned above, see Figs. 3 and 4), we discuss here those concerning the optical properties of the Laue lenses, in particular the on-axis and off-axis responses, the lens angular resolution and its field of view (FOV).

We show in Fig. 5 the expected Point Spread Function (PSF) of the lens with 80 m focal length in the case of an on-axis X-ray source, while in Fig. 6 we show the expected PSF when three sources are in the lens Field of View (FOV), one on-axis and two off-axis. As can be seen, in the case of off-axis sources the PSF has a ring shape with center in the lens focus, an inner radius which increases with the offset angle and a disuniform width with azimuth. This disuniformity gives information on the sky direction of the X-ray source. From the radial distribution of the focused photons due to sources with different offset (see Fig. 7), it is possible to derive the angular resolution of the lens. Conservatively, it results to be about 2 arcmin, i.e., about two times larger than that of the crystal mosaic spread assumed (1 arcmin).

From the numerical simulations it results that the number of photons focused by the lens does not significantly vary from an on-axis source and to an off-axis source. Thus the FOV of the lens in principle seems to be

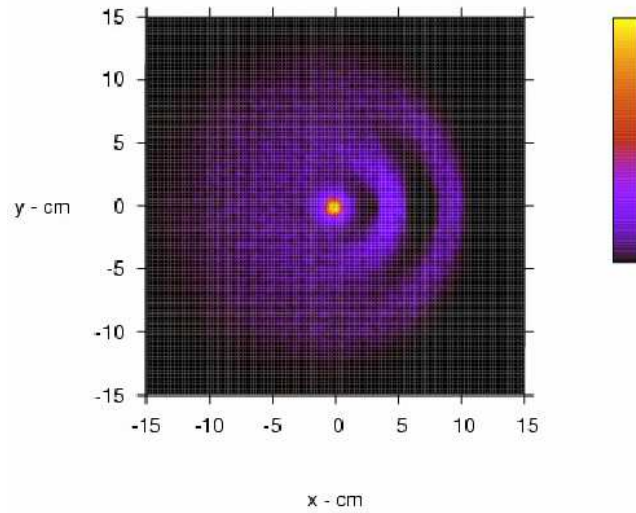


Figure 6. Point spread function of a lens with 80 m focal length in the case of the observation of three sources, one on-axis and the other two offset by 2 and 4 arcmin. The energy band is 150–600 keV.

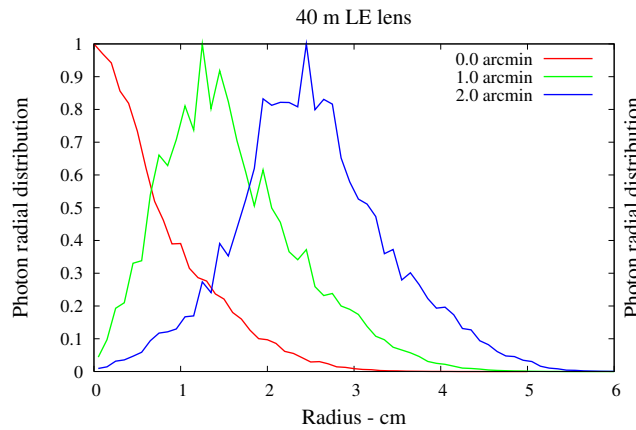


Figure 7. Radial distribution of the photons at different offset angles for 40 m focal length.

determined by the detector radius. However, given that focused photons from sources at increasing offset spread over an increasing area, the detector radius is determined by the lens sensitivity.

2.3. Results from experimental activity

To test the reliability of our feasibility study, we have performed many reflectivity measurements of mosaic crystal samples of Cu(111). The samples, with various thicknesses and mosaic spreads, were provided by the Institute Laue Langevin (ILL), that has developed the technology for growing large single crystals of Copper with a small mosaic spread.⁸ The crystal samples were tested at the Ferrara X-ray facility.^{9,10} Using a pencil beam of polychromatic X-rays, reflectivity curves were derived in an array of positions of the crystal cross section to study the uniformity of the mosaic properties. Results of these measurements have been reported and discussed by Pellicciotta et al.⁵

The reflectivity curves were fit with the theoretical model function derived by Zachariassen.¹¹ In most cases the results were found satisfactory. Figure 8 shows a typical result of the fitting analysis. Evidence of crystal

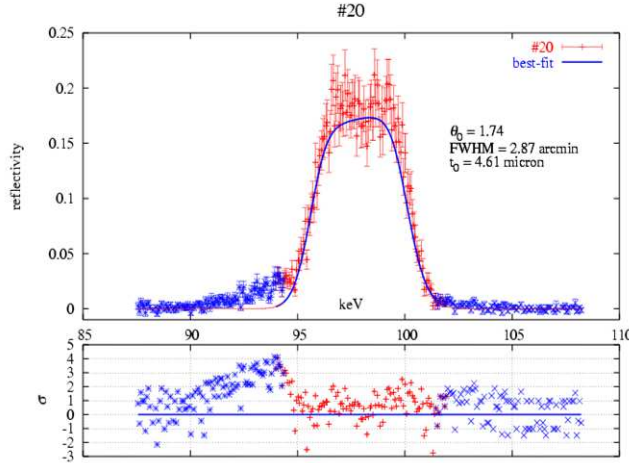


Figure 8. Example of measured reflectivity profile. Also shown is the best fit model with the model function derived by¹¹ and the residuals to the model (bottom panel). Reprinted from Pellicciotta et al.⁵

inhomogeneity was observed near the crystal boundaries, mainly due to the crystal cutting procedure which perturbs the mosaic structure. Given that, for our goals, the crystals should be as homogeneous as possible, the cutting procedure requires further refinement. In spite of that, the measurements results obtained substantially confirm the expectations of our feasibility study.

We are now developing a Demonstration Model (DM) to establish the best crystal assembling technique of the lens. The DM is a sector of the lens and is shown in Fig. 9. It is composed of 30 mosaic crystal tiles with 3 arcmin spread and 15×15 mm² front surface. We have already built some mock-up models, made of polycrystalline copper, and we are now starting to build a model made of true mosaic crystals. The picture of the first mock-up assembly during the testing of the crystal positioning accuracy is shown in Fig. 10. After the DM, we plan to build a Prototype Model (PM), like the entire lens shown in Fig. 9. The realization of the PM will be a good benchmark about our capability of scaling the assembling technology to larger lenses. Both DM and PM will be tested at the Ferrara X-ray facility which is now being extended for this project.¹²

3. STUDY OF POSSIBLE LENS CONFIGURATIONS FOR THE GRI MISSION

On the basis of the feasibility study above summarized and the test results of the mosaic crystal samples of Cu(111), we are now investigating different configurations of Laue lenses that meet the requirements of the GRI mission now under study. For a description of the science goals of this mission and its sensitivity requirements see Knoedlseder.¹³ Shortly, the main requirement of this mission is an unprecedented sensitivity for the study of the continuum emission from about 100 keV to 600 keV, and for the detection of both 511 keV annihilation lines and nuclear lines in the range from 800 to 900 keV. For an observation time of $T = 10^5$ s, the spectrum determination sensitivity should be of the order or better than 10^{-7} photons/(cm² s keV) at 300 keV, while the sensitivity to nuclear lines should be of the order of 10^{-6} photons/(cm² s) or better. The energy passband of the mission is required to be extended to lower energies with an X-ray monitor capable of determining the X-ray spectra of the gamma-ray target sources down to ≤ 20 keV. The baseline monitor assumed is a coded mask telescope, with the mask to be located in the hole left free by the inner lens, i.e., the lens devoted to the nuclear lines (Nuclear Line Lens, NLL).

We have assumed lens sizes compatible with the fairing of the Russian launcher Soyuz (maximum diameter of 380 cm and height of 925 cm). The best focal length that meets the continuum and nuclear line sensitivity requirements, is resulted to be of 75 m. A lower focal length would privilege the continuum sensitivity, while a higher focal length would privilege the nuclear line sensitivity.

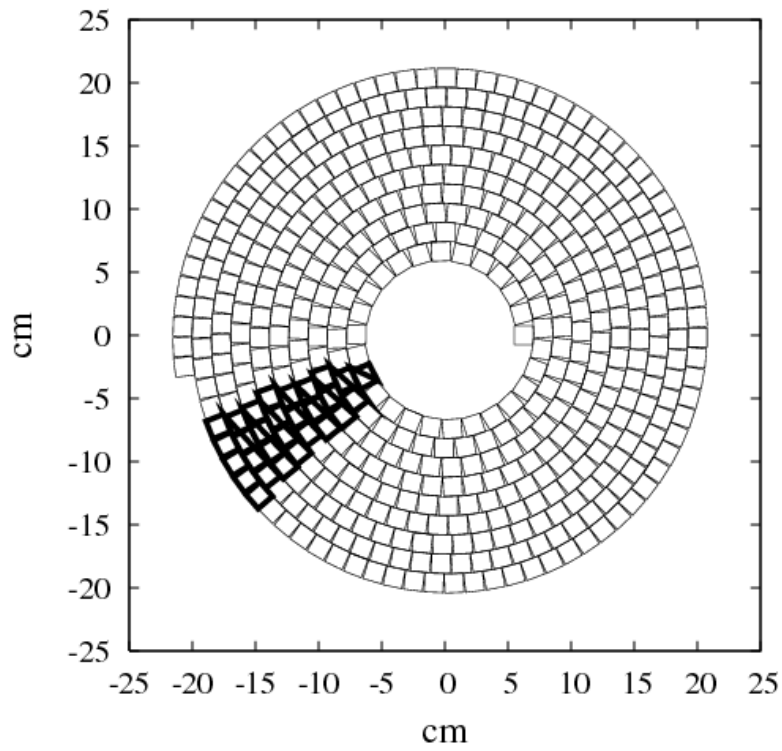


Figure 9. Scheme of a lens of 210 cm focal length made of Cu(111) mosaic crystal tiles disposed according to an Archimedes' spiral. Also shown, in bold-faced, is the DM we are developing to establish the crystal assembling technique.

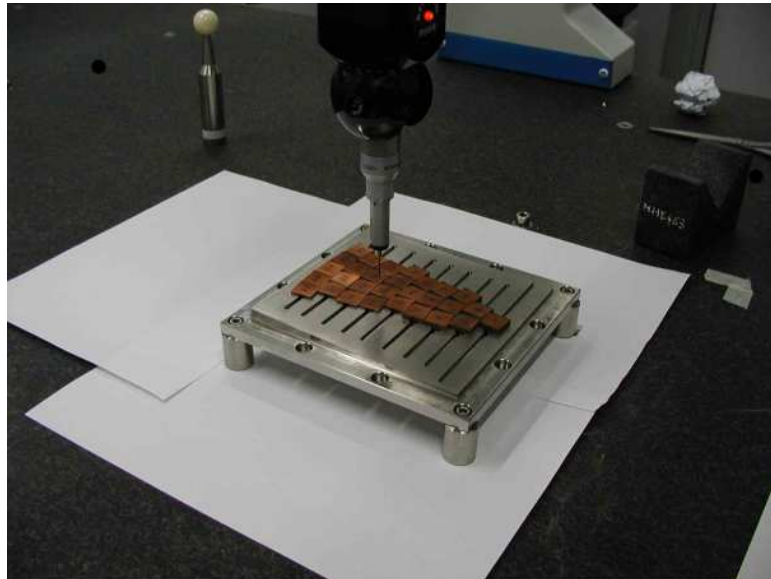


Figure 10. Picture of the first DM mock-up during the testing phase of the positioning accuracy with a profilometer.

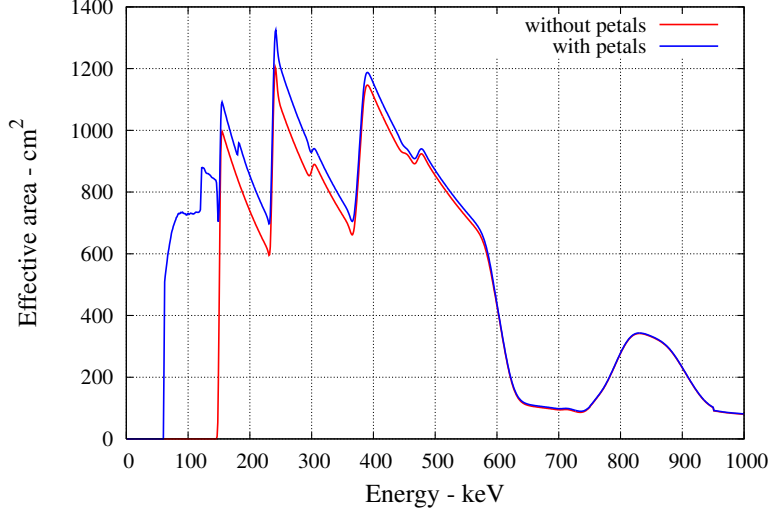


Figure 11. Effective area of a broad energy passband lens (BEL) made of Ge(111) and Cu(111) to cover the 150 to 600 keV plus a nuclear line lens (NLL) to cover the 800 to 900 keV energy band (see features in Table 1). Also shown is the effective area of the same lens, with energy passband extended down to 60 by means of the addition of a 4 petal-like lens (see features in Table 1).

As lens materials we have assumed only Cu(111) and Ge(111), which at the moment are available with a mosaic structure. Other candidate mosaic crystals, like those shown in Fig. 2, could become available in the next future.

In spite that Cu(111) shows higher reflectivity than Ge (111) (see Fig. 2), due to its low lattice spacing (2.087 \AA), a lens based on this material with 75 m focal length has an energy threshold (236 keV) that does not meet the GRI requirements. These requirements can be met by a Ge(111) lens (energy threshold of 150 keV), which however is less efficient. In the first two columns of Table 1 we show the main features of two lenses suitable to study the continuum emission (continuum lenses), one based on Ge (111) (Low Energy Lens, LEL) and the other based on Cu (111) (High Energy Lens, HEL). It is apparent the better effective area (@ 300 keV) of the Cu lens with respect to the Ge lens, which however allows a lower energy passband.

To get a Broad Energy Lens (BEL) with a passband from 150 to 600 keV, we have assumed a lens partly covered with Ge(111) and partly with Cu(111), with an unavoidable loss of effective area at low energies with respect to the HEL/Cu (see Table 1). Figure 11 shows the effective area of the BEL plus that of the NLL, which is designed for the 800–900 keV passband. The NLL features are shown in Table 1. For the latter lens, unlike a mosaic spread of 1 arcmin, we have assumed 40 arcsec, to decrease the half power radius of the focused photon spot (see Table 1).

We have also investigated the possibility of extending the energy passband of the BEL from 150 keV down to 60 keV, through the addition of a petal-like lens, to be deployed in orbit. In Table 1 we show the main features this lens, which is made of 4 petals of 100 cm width. The effective area of this lens and its impact to higher energies is shown in Fig. 11. Such additional lens could become mandatory if the X-ray monitor does not meet the sensitivity requirements.

The expected 3σ sensitivity to the continuum emission of the BEL plus NLL with or without petals is shown in Fig. 12. We have assumed an exposure time of 10^6 s, and a ratio $R = \sqrt{B/\eta_d} = 7 \times 10^{-3}$. To get this figure, it is crucial to have a low detector background and a high detection efficiency. The expected sensitivity to the 511 keV (847 keV) line is given by $I_{511} = 1.9 \times 10^{-7}$ photons $\text{cm}^{-2} \text{ s}^{-1}$ ($I_{847} = 1.4 \times 10^{-6}$ photons $\text{cm}^{-2} \text{ s}^{-1}$), for an assumed ratio $R = 1 \times 10^{-2}$ and line width of 3 keV (25 keV).

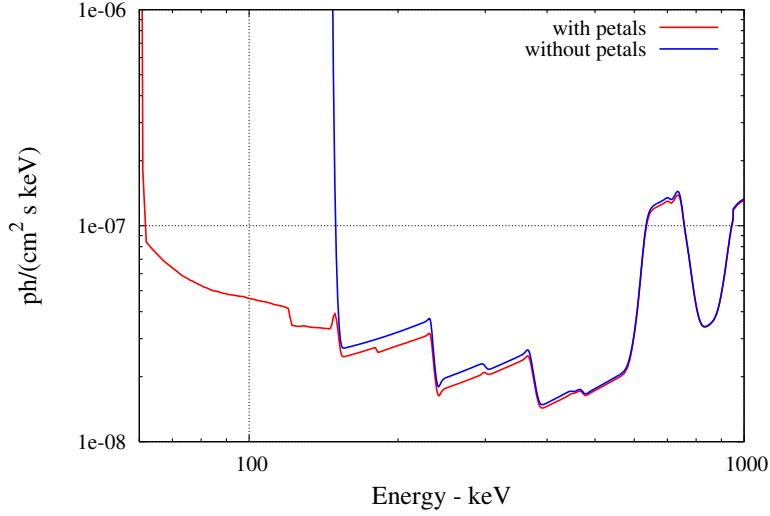


Figure 12. Expected sensitivity at a 3σ confidence level of the BEL plus NLL lenses with (lower line) or without (upper line) the addition of a petal-like lens with 4 petals of 100 cm width (see details in the text and in the Table 1).

Table 1. Main features of the different Laue lens configurations

Parameter	LEL/Ge	HEL/Cu	NLL/Cu	BEL/Ge+Cu	Petals/Ge
Focal length (m)	75	75	75	75	75
Nominal passband (keV)	150–385	236–600	800–900	150–600	60–150
Inner radius (cm)	74	74	50	74	193
Outer radius (cm)	190	190	57	190	475
Crystal material	Ge(111)	Cu(111)	Cu(111)	Ge(111) + Cu(111)	Ge(111)
Mosaic spread (arcmin)	1	1	0.67	1	1
Tile cross section (mm ²)	10 × 10	10 × 10	10 × 10	10 × 10	10 × 10
Tile thickness (mm)	optimized	optimized	9	optimized	optimized
No. of tiles	89197	89197	2242	31865 (Ge), 57191 (Cu)	108952
Lens total surface (m ²)	9.62	9.62	0.235	9.62	11.3
Filling factor	0.93	0.93	0.95	0.95	0.96
Crystal weight (kg)	115	175	18	200	58
Effective area (cm ²) @ 300 keV	862	1652	-	870	60
Effective area (cm ²) @ 511 keV	160	932	-	854	17
Half power radius(mm)	14	14	9	15	15

4. CONCLUSIONS

The development status of a Laue lens project has been outlined. After a design phase of a broad band Laue lens based on mosaic crystals, we have passed to an experimental phase with the test of mosaic crystals of Cu(111). All the results obtained have been very promising. We are now developing a first lens prototype. The Monte Carlo simulations show interesting expectations of the Laue lenses designed, with an expected angular resolution of about 2 arcmin and a field of view that depends on the focal detector radius and instrument sensitivity. We have investigated possible lens configurations for the GRI mission, finding that the best compromise for getting an unprecedented sensitivity for the continuum spectrum determination in the 150–600 keV and for the emission line detection (511 keV and lines in the band from 800 to 900 keV) is a set of two lenses of 75 m focal length, one made of Ge(111) and Cu(111) that covers the band from 150–600 keV, and the other made of Cu(111) with 800–900 keV passband. The lens passband can be extended to 60 keV with the addition of a petal-like lens. This lens is also compatible with a Soyuz launcher fairing, but needs to be deployed in orbit. This deployment capability is estimated to be feasible.

ACKNOWLEDGMENTS

We acknowledge the support by the Italian Space Agency and Italian Institute of Astrophysics (INAF). This research was also possible thanks to received Descartes Prize 2002 of the European Committee.

REFERENCES

1. F. Frontera, et al., "Exploring the hard X-/gamma-ray continuum spectra with Laue lenses", *Proc. 39th ESLAB Symposium*, ESA Publications Division, **SP-588** pp. 323-326, 2006 (astro-ph/0507175).
2. P. von Ballmoos et al., "MAX: a gamma-ray lens for nuclear astrophysics", *Proc. SPIE*, **5168**, pp.482–491, 2004.
3. A. Pisa et al., "Feasibility study of a Laue lens for hard X-rays for Space Astronomy", *Proc. SPIE*, **5536**, pp. 39–48, 2004. (astro-ph/0411574)
4. A. Pisa et al., "Development status of a Laue lens for high energy X-rays (>60 keV)", *Proc. SPIE*, **5900**, pp.350–359, 2005.
5. D. Pellicciotta et al., "Laue lens development for hard X-rays (>60 keV)", *IEEE Trans. Nucl. Sci.*, **53**, 253–258, 2006. (astro-ph/0511490)
6. A. Pisa et al., "Optical properties of Laue lenses for hard X-rays (>60 keV)", *Exper. Astron.*, in press, 2006.
7. F. Frontera et al., "HAXTEL: a Laue lens telescope development project for a deep exploration of the hard X-ray sky (>60 keV)", *Exper. Astron.*, in press, 2006.
8. P. Courtois, B. Hamelin, and K.H. Andersen, "Production of copper and Heusler alloy Cu₂MnAl mosaic single crystals for neutron monochromators", *Nucl. Instr. Meth.*, **529**, 157–161, 2004.
9. G. Loffredo et al., "X-ray facility for the ground calibration of the X-ray monitor JEM-X on board INTEGRAL", *Astron. & Astrophys.*, **411**, L239, 2003.
10. G. Loffredo et al., "The X-ray facility of the Physics Department of the Ferrara University", *Exper. Astron.*, **10**, 1-11, 2004.
11. Zachariasen, W. H., *Theory of X-rays Diffraction in Crystals*, Wiley, New York, 1945.
12. G. Loffredo et al., "The Ferrara hard X-ray facility for testing/calibrating hard X-ray focusing telescopes", *Exper. Astron.*, in press, 2006.
13. J. Knodlseder, *GRI: the Gamma Ray Imager mission*, this issue, 2006